MOLECULAR PHYSICS, 20 JULY–10 AUGUST 2004, VOL. 102, NO. 14–15, 1605–1614

Taylor & Francis
Taylor & Francis Group

Determination of the structure of 7-azaindole in the electronic ground and excited state using high-resolution ultraviolet spectroscopy and an automated assignment based on a genetic algorithm

MICHAEL SCHMITT[1]*, CHRISTIAN RATZER[1], KARL KLEINERMANNS[1] and W. LEO MEERTS[2]*

[1]Heinrich-Heine-Universität, Institut für Physikalische Chemie, D-40225 Düsseldorf, Germany
[2]Department of Molecular and Laser Physics, NSRIM, University of Nijmegen, NL-6500 GL Nijmegen, The Netherlands

(*Received 23 February 2004; accepted 7 April 2004*)

The rotationally resolved electronic spectra of four different isotopomers of 7-azaindole (1*H*-pyrrolo(2,3-*b*)pyridine) have been measured in order to obtain the geometric structure in the electronic ground and excited state. The electronic origins of the rotationally resolved UV spectra overlap strongly and an assigned fit to single rovibronic lines is hardly possible. We performed an automatized fit based on the genetic algorithm to assign all four spectral components simultaneously and extract the molecular constants. The resulting inertial parameters were used to determine the structure of 7-azaindole in the ground and electronically excited state. It was found that the pyridine moiety expands on electronic excitation, while the pyrrole ring showed only minor geometric changes. From the hybrid-type spectra of three isotopomers, the direction of the $\tilde{A}^1A'(\pi\pi^*)$–$\tilde{X}^1A'$ transition dipole moment for the transition was found to be $-21°$. Evaluation of the individual line shapes yielded an excited state lifetime of 2.55 ns for 7-azaindole.

1. Introduction

7-Azaindole (7AI) has been subject to numerous experimental and theoretical studies in the last decades, mainly because the 7-azaindole dimer serves as a model system for tautomeric processes in DNA base pairs [1]. Furthermore, 7-azaindole is the chromophore of the amino acid analog 7-azatryptophan, which is used to replace tryptophan in proteins. The absorption and emission of 7AI are red-shifted compared with tryptophan and show a single exponential decay, which makes 7AI a good alterative in the optical probing of proteins [2].

7AI (see figure 1 for atomic numbering) exists in two tautomeric forms: 1*H*-pyrrolo(2,3-*b*)pyridine, in which the H atom is connected to the N atom of the pyrrole moiety, and 7*H*-pyrrolo(2,3-*b*)pyridine, with the H atom at the N of the pyridine site. While the barrier separating the two tautomers is quite high in the electronic ground state, it decreases by a factor of 10 in the first electronically excited state [3], which gives rise to intramolecular excited-state proton transfer (ESPT). The geometry of both tautomers and the transition state connecting them has been determined at various levels of theory for different electronic states [4–7].

From an experimental and theoretical point of view it is well established that the lowest electronically excited singlet state is of $\pi\pi^*$ character with no or little mixing with the $n\pi^*$ state. However, the energetic ordering of the electronically excited states remains controversial. According to the CIS calculations of Shukla and Mishra [4] the lowest $\pi\pi^*$ state is followed by a $n\pi^*$ state. Ilitch proposed the same energetic ordering of electronically excited states on the basis of an UV/vis study in an argon matrix and its comparison with INDO/S1 calculations [3]. However, CASSCF calculations by Borin and Serrano-Andrés [7] predict the energetic ordering of excited states in 7-azaindole to be the same as in indole. The lowest singlet state S_1 is ^1L_b and the next lowest ^1L_a according to Platts nomenclature.

The structure of 7AI in the electronic ground state was investigated by Caminati *et al.* using microwave spectroscopy [8]. They obtained the rotational constants of the normal isotopomer and of the N–D monodeuterated species. From Stark effect measurements, they obtained a value for the dipole moment of $\mu_a = 1.49$ and $\mu_b = 0.77$ D.

*Authors for correspondence. e-mail: mschmitt@uni-duesseldorf.de/Leo.Meerts@sci.kon.nl

Molecular Physics ISSN 0026–8976 print/ISSN 1362–3028 online © 2004 Taylor & Francis Ltd
http://www.tandf.co.uk/journals
DOI: 10.1080/00268970410001725747

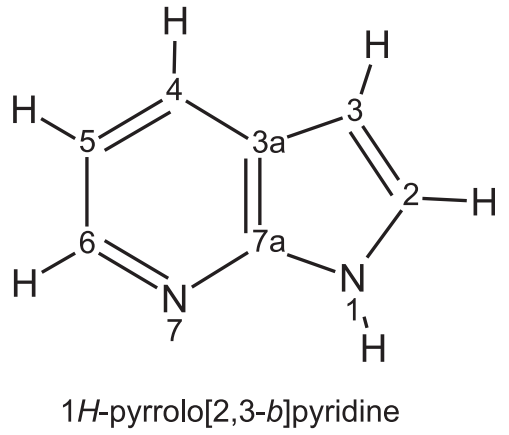

1*H*-pyrrolo[2,3-*b*]pyridine

Figure 1. Atomic numbering of 7AI (1*H*-pyrrolo[2,3-*b*]pyridine) and its isotopomers.

The S_1–S_0 system around 298 nm was assigned as the $\tilde{A}\,^1A'(\pi\pi^*)$–$\tilde{X}\,^1A'$ transition by Hassan and Hollas [9]. They determined the rotational constants in both electronic states and the transition dipole moment hybrid ratio from a rotational band contour analysis of the 298 nm band system. The expansion of the pyridine ring upon electronic excitation was discussed on the basis of the rotational constants. Furthermore, the electronic origin of the same band system was investigated by high-resolution LIF spectroscopy by Nakajima *et al.* [10]. In that study, they determined the rotational constants of both states of the monomer and of some hydrogen-bonded clusters. Huang *et al.* reported a fluorescence lifetime of 5.7 ns after excitation of the electronic origin of the lowest $\pi\pi^*$ state [11]. They determined the lifetimes of several vibronic bands up to 937 cm^{-1} above the electronic origin and excluded coupling of the ^1L_b with a nearby $n\pi^*$ state.

The orientation of the transition dipole moment (TDM) of the lowest $\pi\pi^*$ state has been determined both theoretically and experimentally. Catalan and Perez obtained a value of $+7.5^\circ$ using the CNDO/S method [12]. Ilitch reports an angle of $+0.8^\circ$ based on INDO/S1 calculations [3]. From a CASSCF study, Borine and Serrano-Andrés obtained a value of $+27^\circ$ for the ^1L_b state [7]. The evaluation of a rotational contour by Hassan and Hollas gave an ab-hybrid with 93% a- and 7% b-type, resulting in an angle of $\pm 15^\circ$ [9]. Nakajima *et al.* obtained a value of $\pm 21^\circ$ from a rotational resolved LIF spectrum [10]. In these experimental studies it is only possible to determine the square of the TDM, leaving the sign (and therefore the direction) undetermined.

In the present publication (paper I) we report a study of the geometry of the 7AI monomer in the ground and electronically excited state by means of the rotationally resolved laser-induced fluorescence spectroscopy of four different isotopomers. These isotopomers comprise (i) the normal isotopomer 1*H*-pyrrolo(2,3-*b*)pyridine (7AI); (ii) 1*H*-pyrrolo[2,3-*b*]pyridine-1-d_1, which is deuterated at the pyrrolic NH group (in the following we will use the abbreviation 7AI[ND] for this isotopomer); (iii) the singly deuterated isotopomer 1*H*-pyrrolo[2,3-*b*]pyridine-3-d_1, which is deuterated at the C_3H position (see figure 1) and will be denoted 7AI[CD] in the following; and (iv) deuteration at NH and C_3H leads to doubly deuterated 1*H*-pyrrolo[2,3-*b*]pyridine-1,3-d_2 (7AI[ND][CD]). The molecular parameters of the strongly overlapping spectra are fitted using a genetic algorithm approach, described by Hagemann *et al.* [13] and Meerts *et al.* [14]. From the inertial parameters, the geometries of the electronic ground and excited state and the absolute direction of the TDM are determined. This investigation precedes a Franck–Condon analysis of the same system, which will be presented in a forthcoming paper (paper II).

2. Experimental

The experimental setup for the rotationally resolved LIF is described elsewhere [15]. Briefly, it consists of a ring dye laser (Coherent 899-21) operated with Rhodamine 110, pumped with 6 W of the 514 nm line of an Ar^+-ion laser. The light is coupled into an external folded ring cavity (Spectra Physics) for second harmonic generation (SHG). The molecular beam is formed by expanding 7AI, seeded in 600 mbar of argon, through a 70 μm hole into the vacuum. The molecular beam machine consists of three differentially pumped vacuum chambers that are connected linearly by skimmers (1 mm and 3 mm, respectively) in order to reduce the Doppler width. The molecular beam is crossed at right angles in the third chamber with the laser beam 360 mm downstream of the nozzle. The resulting fluorescence is collected perpendicular to the plane defined by the laser and the molecular beam by an imaging optics setup consisting of a concave mirror and two plano-convex lenses. The resulting Doppler width in this setup is 25 MHz (FWHM). The integrated molecular fluorescence is detected by a photo-multiplier tube, the output of which is discriminated and digitized by a photon counter and transmitted to a PC for data recording and processing. The relative frequency is determined with a quasi-confocal Fabry–Perot interferometer with a free spectral range (FSR) of 149.9434(56) MHz. The FSR was calibrated using the combination differences of 111 transitions of indole for which the microwave transitions are known [16, 17]. The absolute frequency was determined by recording the iodine absorption spectrum and comparing the transitions with the tabulated lines [18].

7AI was purchased from Fluka and was used without further purification. 7AI[ND] was prepared from 7AI by

passing 20 mbar D_2O seeded in argon gas over the solid sample and expanding the mixture into the vacuum. 7AI[CD] and 7AI[ND][CD] were obtained by refluxing 7AI three times with an excess of DCl in D_2O (38%) and subsequent removal of the solvent. This resulted in a 50:50 mixture of mono- and bideuterated species. The number of H atoms exchanged by deuterium was checked using a time-of-flight mass spectrometer. No deuterated species higher than d_2 were found. The electronic origins of all four isotopomers are only slightly shifted (approx. $0.5\,cm^{-1}$), with an energetic ordering of 7AI, 7AI[ND], 7AI[CD], and 7AI[ND][CD].

3. Results

Figure 2 shows the high-resolution LIF spectrum of the electronic origin of 7AI at $34630.74\,cm^{-1}$. The spectrum was automatically assigned using the genetic algorithm (GA)-based fit described in [13, 14]. The GA library PGAPack, version 1.0, which can run on parallel processors, was used [19]. The calculations were performed with four processors of a SUN UltraSPARC 333 MHz and a 2.6 GHz PC with two processors under Linux. The genetic algorithm uses concepts copied from natural reproduction and selection processes. For a detailed description of the GA, the reader is referred to the original literature on evolutionary or genetic algorithms [20–22].

The molecular parameters are binary encoded using a Gray Code [23], each parameter representing a gene. A vector of all genes, which contains all molecular parameters, is called a chromosome. In an initial step, the values of all parameters are set to random values between lower and upper limits which have to be chosen by the user. Table 1 shows an example input for the GA for 7AI. A total of 300–500 chromosomes are randomly generated, forming a population.

The solutions are evaluated by a fitness function, which is a measure of the quality of the individual solutions. A proper choice of the fitness function is of vital importance for the success of GA convergence. The fitness function F_{fg} has been defined as [13, 14]

$$F_{\mathbf{fg}} = \frac{(\boldsymbol{f},\boldsymbol{g})}{\|\boldsymbol{f}\|\|\boldsymbol{g}\|}. \tag{1}$$

Here, $\boldsymbol{f}$ and $\boldsymbol{g}$ are the vector representations of the experimental and calculated spectrum, respectively, and the inner product $(\boldsymbol{f},\boldsymbol{g})$ is defined with the metric $\boldsymbol{W}$ as

$$(\boldsymbol{f},\boldsymbol{g}) = \boldsymbol{f}^{\mathrm{T}}\boldsymbol{W}\boldsymbol{g}, \tag{2}$$

Table 1. Input parameters and limits for the genetic algorithm fit of the spectrum of 7-azaindole.

	Lower	Upper	Guess
A'' (MHz)	3900	4100	4000
B'' (MHz)	1650	1750	1700
C'' (MHz)	1150	1250	1200
ν_0 (MHz)[a]	25,000	27,000	26,000
T (K)	1	4	2
θ (deg)[b]	0	60	20
$\Delta A'$ (MHz)	−200	200	−150
$\Delta B'$ (MHz)	−100	100	0
$\Delta C'$ (MHz)	−100	100	−20

[a]Relative to the beginning of the scan.
[b]The angle θ is defined as the angle between the TDM and the inertial a axis.

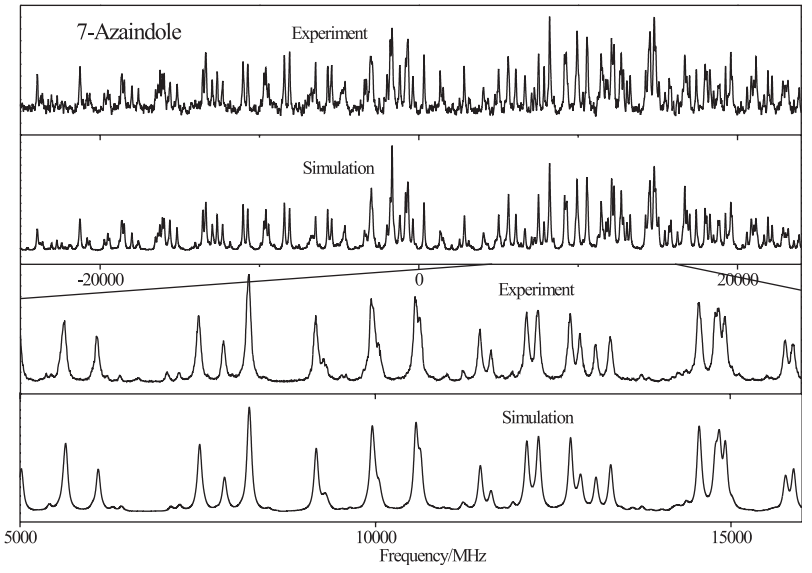

Figure 2. Rotationally resolved LIF spectrum of 7AI. The frequency is given relative to the electronic origin.

and the norm of $\boldsymbol{f}$ as $\|\boldsymbol{f}\| = \sqrt{(\boldsymbol{f},\boldsymbol{f})}$; similarly for $\boldsymbol{g}$. For $w(r)$ we used a triangle function [13] with a base width of Δw:

$$w(r) = \begin{cases} 1 - |r|/(1/2\Delta w) & \text{for } |r| \leqslant 1/2\Delta w, \\ 0 & \text{otherwise.} \end{cases} \quad (3)$$

One optimization cycle, including evaluation of the fitness of all solutions, is called a generation. Pairs of chromosomes are selected for reproduction and their information is combined via a crossover process. As crossover combines information from the parent generations, it basically explores the error landscape. The value of a small number of bits is changed randomly. This process is called mutation. To avoid degradation of already good solutions, the best solutions within a generation are excluded from mutation.

For the simulation of the rovibronic spectra, a rigid asymmetric rotor Hamiltonian was employed [24]. The parameters to be determined by the GA are the three rotational constants A, B and C for each electronic state, the origin frequency ν_0 of the vibronic band and line intensity determining parameters such as rotational temperature, transition dipole moment orientation and line shape parameters (see Section 3.1). The rotational constants of 7AI obtained from the GA fit of the spectrum given in figure 2 are reported in table 2. For the electronic ground state, the more accurate values from the microwave investigations of Caminati *et al.* [8] were taken.

Soft deuteration, by adding 20 mbar D_2O to the Ar seed gas prior to expansion, resulted in the spectrum shown in figure 3. Apparently, a second band emerges, which can be assigned to the 7AI[ND] isotopomer. Both bands were fit together using the GA. The molecular constants of the first spectrum, such as rotational constants, origin frequency, and Lorentzian width, were fixed, whereas the global parameters for the complete fit, such as temperature(s), weights, baseline, relative intensity of both spectra, etc., were allowed to vary. As for 7AI, the ground state rotational constants of 7AI[ND] were fixed to the MW values of Caminati *et al.* [8]. The resulting rotational constants for 7AI[ND] for both electronic states are listed in table 2. The frequency of the electronic origin is given as the difference to the origin of 7AI, because this number can be determined more accurately than the absolute frequency.

Higher deuteration grades were obtained by the method described in Section 2. Figure 4 shows the resulting high-resolution spectrum. Two new bands appeared to the blue of the two isotopomers already described. From the mass spectrum of the deuterated substance we know that the highest deuteration grade was d_2. Thus, one of the new bands belongs to a d_2 isotopomer, and the other to a d_1 isotopomer, distinct from 7AI[ND]. We fitted the complete spectrum with the parameters of the first two bands fixed to the above-determined values. The GA succeeded in finding the rotational constants for the other two isotopomers. Their values are given in table 2. Comparison with the predicted rotational constants, obtained from the *ab initio* structure for all possible singly and doubly deuterated isotopomers, immediately showed that only 1*H*-pyrrolo[2,3-*b*]pyridine-3-d_1 (7AI[CD]) and 1*H*-pyrrolo[2,3-*b*]pyridine-1,3-d_2 (7AI[ND][CD]) match the experimentally determined rotational constants.

Table 2. Molecular parameters of the electronic origin band of 7-azaindole as obtained from the genetic algorithm fit. All values are given in MHz.

	7AI	7AI[ND]	7AI[CD]	7AI[ND][CD]
A''	3928.93(2)[a]	3807.60(3)[a]	3794.95(60)	3674.46(24)
B''	1702.629(3)[a]	1684.722(2)[a]	1678.73(16)	1662.45(15)
C''	1188.128(5)[a]	1168.241(2)[a]	1164.10(8)	1144.89(5)
ν_0[b]	0	27553.67(12)	51934.78(98)	80640.38(39)
ΔA	−183.47(11)	−173.77(6)	−172.11(10)	−162.50(8)
ΔB	1.24(5)	−0.48(3)	−0.62(4)	−0.07(5)
ΔC	−16.62(3)	−16.95(2)	−16.89(7)	−16.21(1)

[a]Values for the electronic ground states from [8].
[b]Relative to the electronic origin of 7AI at 34630.74 cm^{-1}.

The isotopic shift of the four spectra is relatively small compared with other spectra of aromatic molecules. These amount to 27553.67 MHz (0.92 cm^{-1}), 51934.78 MHz (1.73 cm^{-1}) and 80640.38 MHz (2.69 cm^{-1}), respectively. As the origin shift depends only on the difference in zero-point energy, virtually equal vibrational frequencies for the NH and CH stretching vibrations in both electronic states are expected.

3.1. *Orientation of the transition dipole moment and excited state lifetime*

Since the GA performs a line shape fit of the complete spectrum, much better information on the line width is gathered than from a line shape fit to a few individual lines. In order to obtain the relevant parameters that determine the intensities in the spectrum, we performed a second GA fit with a reduced search range and the weight function width $\Delta w = 0$. This resulted in improved values for the angles θ and ϕ, which are associated with the components of the transition dipole moment by

$$\begin{aligned} \mu_a &= \mu \sin\phi \cos\theta, \\ \mu_b &= \mu \sin\phi \sin\theta, \\ \mu_c &= \mu \cos\phi. \end{aligned} \quad (4)$$

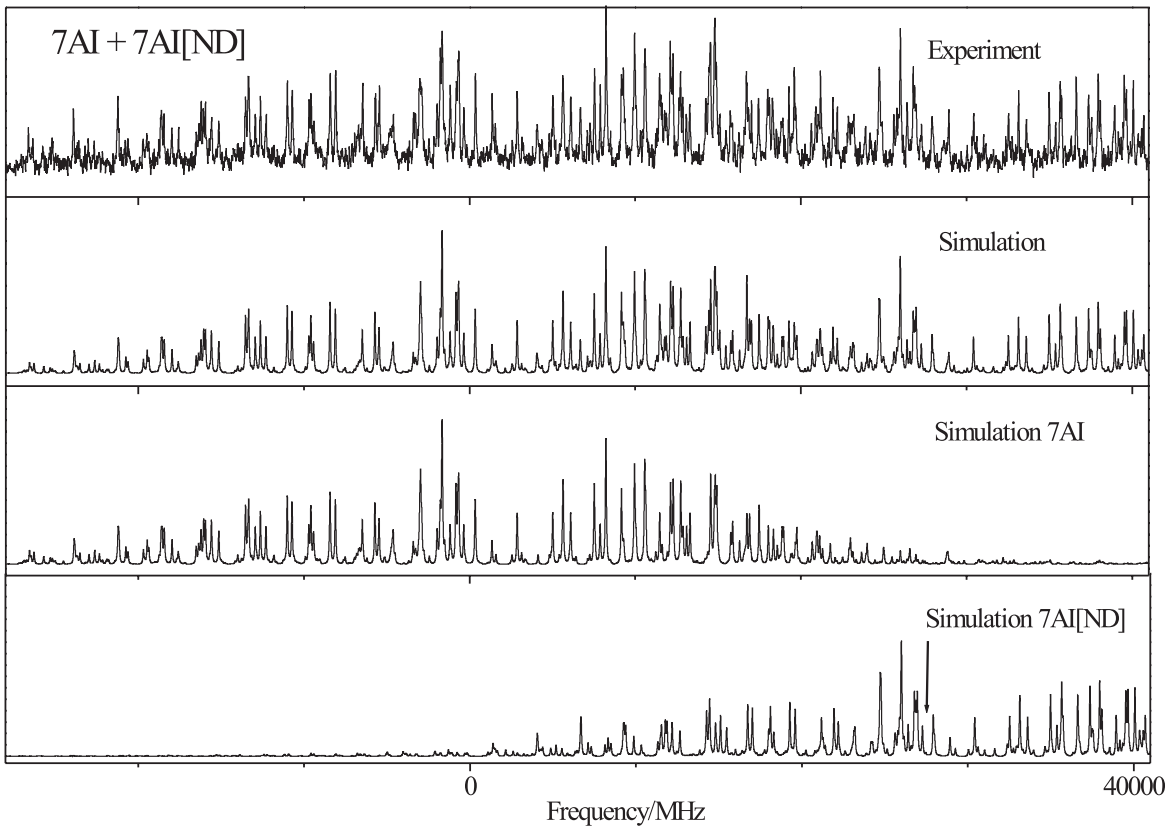

Figure 3. Rotationally resolved LIF spectrum of 7AI and 7AI[ND]. The upper trace gives the experimental spectrum, the second trace the simulation, using the best fit parameters. The following traces show simulations of the individual spectra of 7AI and 7AI[ND]. They are given only for clarity; the fit was performed using the overall spectrum. The frequency scale is given relative to the electronic origin of 7AI. The origin of 7AI[ND], which is shifted by 27553.67 MHz, is marked by an arrow in the lowest trace.

Determination of the Lorentzian component of the line width can be improved using the fit of all available intensities. The Gaussian width is fixed to the experimentally determined value of 25 MHz. The temperature dependence of the intensity is described by a two-temperature model [25]:

$$n(T_1, T_2, w) = \mathrm{e}^{-E/kT_1} + w\ \mathrm{e}^{-E/kT_2}, \qquad (5)$$

where E is the energy of the lower state, k is the Boltzmann constant, w is a weighting factor, and T_1 and T_2 are the two temperatures. The resulting temperatures and weights obtained from the individual spectra of the four isotopomers are presented in table 3. T_1, T_2 and w are strongly correlated and are therefore given without uncertainties in table 3. They are merely used to facilitate the intensity fit for low and high J states simultaneously.

The TDM for a transition to the $\pi\pi^*$ state in a planar molecule is located in the molecular plane. As a check, both angles between TDM and the inertial axes, θ and ϕ, were fit, resulting in values for μ_c for all isotopomers well below 1%. In all subsequent fits, the model was therefore restricted to the ab-hybrid type. Only one angle, θ, is needed in this case, which is defined as the angle between the TDM and the inertial a axis. The value of θ for different isotopomers can be used to determine the sign, and therefore the direction of the TDM. Isotopic substitution, which takes place off-axis, results in rotation of the respective inertial axis, but the orientation of the TDM remains the same. If the sign of the angle of the TDM with the inertial a axis is positive, as given by most theoretical studies [3, 7, 12], the angle should increase for the ND tautomer and decrease for the CD tautomer (see figure 5). A rough estimate of the change in θ for the three isotopomers was obtained by calculating the rotation of the inertial axis system, based on the *ab initio* structure. The estimated value of between 1.5° and 2.5° for the a axis rotation shows the necessity of an exact experimental determination of θ and of a reliable fit. A rotation of 2° changes the relative intensities of the a and b lines by only 2.5%. This again shows that only an intensity fit to all lines in the spectrum as performed by the GA is capable of

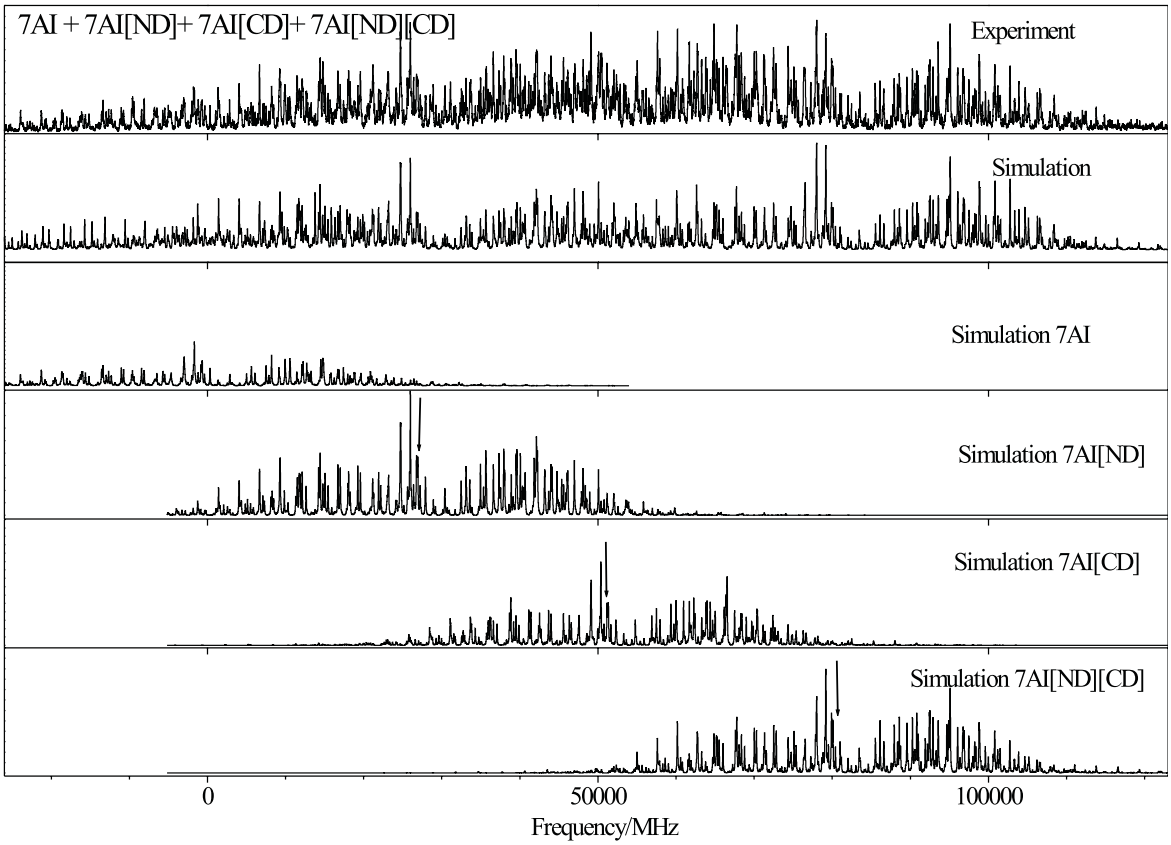

Figure 4. Rotationally resolved LIF spectrum of 7AI, 7AI[ND], 7AI[CD] and 7AI[ND][CD]. The upper trace gives the experimental spectrum, the second trace the simulation, using the best fit parameters. The following traces show simulations of the individual spectra of 7AI, 7AI[ND], 7AI[CD] and 7AI[ND][CD]. They are given only for clarity; the fit was performed using the overall spectrum. The frequency scale is relative to the origin of 7AI. The electronic origins of the other isotopomers are marked by arrows.

Table 3. Parameters that determine the relative intensities in the spectra of 7AI, obtained from a GA fit. For details, see text.

	7AI	7AI[ND]
T_1 (K)	1.62	1.54
T_2 (K)	13.1	19.8
w	0.05	0.10
θ (deg)	21.17(6)	17.29(1)
μ_a^2	0.8910	0.9116
μ_b^2	0.1090	0.0884
$\Delta_{Lorentz}$ (MHz)	62.52(30)	67.96(22)
τ (ns)	2.55(3)	2.34(2)

predicting such tiny changes reliably. A fit to the overlapping spectra of 7AI and 7AI[ND] with the parameters of 7AI fixed at the values determined resulted in values of $\pm 21.2(9)^\circ$ for 7AI and $\pm 17.3(9)^\circ$ for 7AI[ND]. The decrease in the angle θ indicates that the absolute angle in 7AI should be -21°, in contrast to most theoretical studies, which predict a positive angle.

Unfortunately, the hybrid type could not be determined with sufficient accuracy from the spectrum of the four isotopomers shown in figure 4, because, particularly in the region of the third origin (7AI[CD]), spectral congestion is very high due to three overlapping rovibronic bands. Therefore, the uncertainty in the angle θ was larger than the expected effect from rotation of the inertial axes of the CD tautomer, thus prohibiting an independent determination of the sign of TDM orientation from this tautomer.

With a fixed Gaussian contribution of 25 MHz we obtained a Lorentzian contribution of 64 ± 1 MHz for 7AI from a GA analysis. The resulting value of 2.55 ± 0.03 ns for the S_1 state lifetime is less than half of that (5.7 ns) determined by Huang *et al.*, obtained by time-correlated single-photon counting [11]. We checked carefully that, under our experimental conditions, no saturation of the rovibronic lines occurs, which might increase the width of the bands, thus giving a shorter lifetime. The lifetime of 7AI[ND] was determined from the spectrum of the two isotopomers given in figure 3 to be 2.34(2) ns, slightly shorter than that of 7AI.

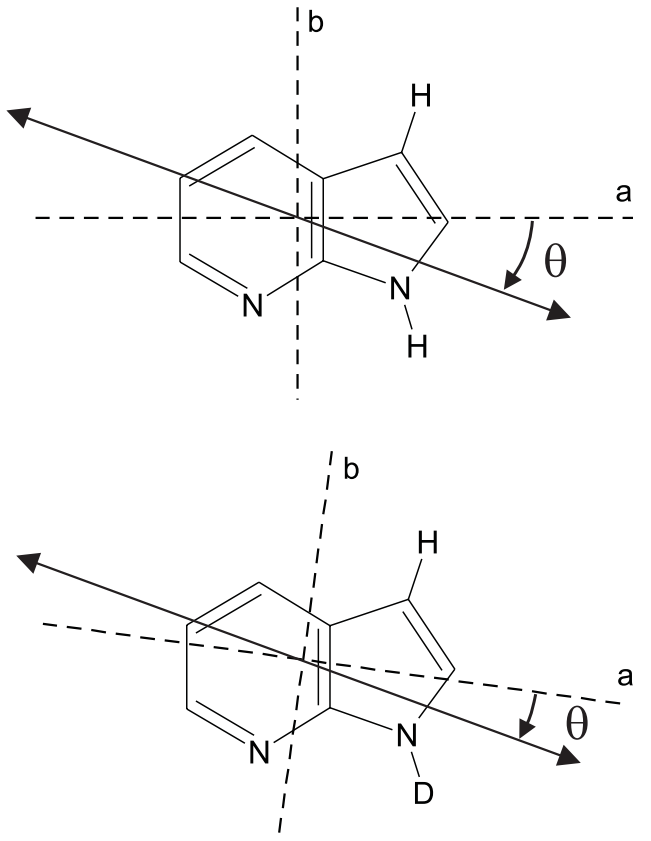

Figure 5. The angle θ between TDM and the inertial a axis for three different isotopomers. The direction shown defines a negative angle. The rotation of the inertial axis system upon deuteration has been exaggerated for reasons of clarity.

The lifetimes of the other two isotopomers could not be determined with sufficient accuracy due to the large spectral congestion (*vide supra*).

3.2. *Determination of the structure*

The program *pKrFit* [26] was used to determine the structure of 7AI in the S_0 and S_1 states.

Of the 12 rotational constants from the four isotopomers, only eight can be used for the fit of the structure, because the other four are linearly dependent. This is a consequence of the planarity of the molecule in both electronic states. Thus, only eight geometric parameters can be fit. Due to the limited number of inertial parameters, we performed a fit limited to the r_0 structure, which neglects the vibrational contributions from the different isotopomers and is based on the assumption

$$I_0^g = I_{\text{rigid}}^g(r_0), \tag{6}$$

where I_0^g are the (experimentally determined) zero-point averaged moments of inertia with respect to the inertial

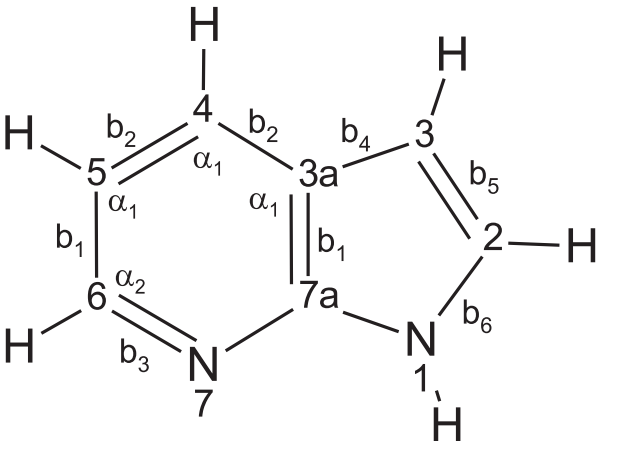

Figure 6. The model structure used for determination of the S_0 and S_1 state geometry.

axes g. The function $I_{\text{rigid}}^g(r_0)$ is calculated from the structural parameter r_0, using rigid-molecule formulae. Thus no vibrational corrections are introduced into the determination of the structure. The limited number of rotational parameters requires a model in which some constraints are placed on the geometry parameters. For the model used, refer to figure 6. The CC bond lengths C7a–C3a and C5–C6 (b_1) and the CC bonds C3a–C4 and C4–C5 (b_2) are set equal and are fit. Furthermore, the C6–N7 bond length in the pyridine moiety (b_3), the CC bond C3a–C3 (b_4), the CC bond C3–C2 (b_5) and the C2–N1 bond of the pyrrole moiety (b_6) are fit independently. The angles formed by atoms C7aC3aC4, C3aC4C5 and C4C5C6 are set equal (α_1) and are fit. The remaining parameter to be fit is the angle between C5C6N7 (α_2). All CH bond lengths are set to 108 pm for the electronic ground state and to 107 pm for the electronically excited state. The NH bond in the pyrrole ring is set to 99 pm for both electronic states. Table 4 shows the deviations between experimental and calculated rotational constants from the structure fit for all four isotopomers in the S_0 and S_1 state. The fitted geometry parameters are given in table 5. The quoted uncertainties were determined by the variances of the experimental inertial parameters and do not contain systematic errors due to the model character of the geometry. These uncertainties might be an order of magnitude larger. Nevertheless, the significance of our conclusions concerning the geometric changes upon electronic excitation are not affected. As can be seen, all bond lengths in the pyridine ring increase upon electronic excitation, whereas the situation in the pyrrole ring is more complex. The CC bond length C3a–C3 (b_4) stays nearly the same, the bond C3–C2 (b_5) decreases and the C6N7 (b_6) bond increases. To summarize, we observe an overall expansion of the pyridine ring and

Table 4. Experimentally determined and fitted rotational constants of the electronic ground and excited state of 7-azaindole, using the model given in figure 6. All values are given in MHz.

	S_0			S_1		
	Exp.	Fit	Diff.	Exp.	Fit.	Diff.
7AI						
A''	3928.93	3929.25	−0.32	3745.46	3745.66	−0.20
B''	1702.629	1702.667	−0.038	1703.87	1704.02	−0.15
C''	1188.128	1187.909	0.218	1171.51	1171.20	0.30
7AI[ND]						
A''	3807.60	3809.52	−1.92	3633.83	3633.99	−0.16
B''	1684.722	1684.766	−0.044	1684.24	1684.47	−0.23
C''	1168.241	1168.150	0.091	1151.29	1150.96	0.32
7AI[CD]						
A''	3794.95	3793.71	1.24	3622.84	3623.92	−1.08
B''	1678.73	1678.93	−0.20	1678.11	1679.62	−1.51
C''	1164.10	1163.86	0.24	1147.21	1147.68	−0.47
7AI[ND][CD]						
A''	3674.46	3674.98	−0.52	3511.96	3512.39	−0.43
B''	1662.45	1662.86	−0.41	1662.38	1662.08	0.29
C''	1144.89	1144.84	0.04	1128.68	1128.21	0.47

Table 5. Comparison of experimentally determined geometry parameters of 7-azaindole in the S_0 and S_1 state. The distances b_i are given in pm, the angles α_i in degrees.

	S_0	S_1	Δ
b_1	142.5(2)	145.3(5)	+2.8
b_2	139.3(1)	140.4(2)	+1.1
b_3	134.5(3)	134.5(4)	0
b_4	144.2(2)	141.9(4)	−2.3
b_5	137.4(2)	133.6(4)	−3.8
b_6	140.6(2)	142.6(4)	+2.0
α_1	118(1)	118(2)	0
α_2	124(1)	127(2)	+3

a slight asymmetric distortion of the pyrrole ring upon electronic excitation. This finding is in good agreement with the results of a Franck–Condon analysis of 7AI and with the results of CASSCF(12/10) calculations, which will be presented in a forthcoming paper. Nevertheless, one should keep in mind that, due to the restricted number of isotopomers, only eight geometry parameters out of a total of 27 independent parameters for a planar molecule with 15 atoms could be included in the fit. Therefore, the calculated geometry is on an equal footing with other geometries that use different restrictions from those made here.

4. Conclusions

The rovibronic spectra of four isotopic species of 7AI were interpreted and assigned automatically using a genetic algorithm approach. A manual assignment to quantum numbers and subsequent fits of the line positions would have been impossible with the strongly overlapping spectra of this molecular system. Using the inertial parameters, the r_0 structure of 7-azaindole has been determined in the S_0 and $S_1(^1L_b)$ state. The main feature of the geometry change upon electronic excitation is an expansion of the pyridine moiety, rather than of the pyrrole ring.

To investigate the excitation, we performed a CIS/6-31G(d,p) calculation, with optimization of the lowest excited state with π symmetry. The differences between these CIS rotational constants and the optimized rotational constants of a HF/6-31G(d,p) calculation for the ground state amount to $\Delta A = -113\,\mathrm{MHz}$, $\Delta B = -8\,\mathrm{MHz}$ and $\Delta C = -16\,\mathrm{MHz}$. Cancellation of the errors between the two electron-uncorrelated SCF methods HF and CIS is known to reproduce the changes in rotational constants upon electronic excitation quite well (see table 6). The ground state rotational constants of 7AI are nearly perfectly reproduced at the MP2 level of theory. CASSCF(12/10) calculations reproduce both the absolute rotational constants for both states, as well as the changes, quite well. Figure 7 shows the molecular orbitals from the CIS calculation that are predominantly involved in this transition. There are two main contributions in this single excitation approximation, one from HOMO − 1 → LUMO + 1 with a coefficient of 0.19, and one from HOMO → LUMO with a coefficient of 0.66. These orbitals are localized mainly in the pyridine ring, thus explaining qualitatively the observed predominant geometry changes in the six-membered

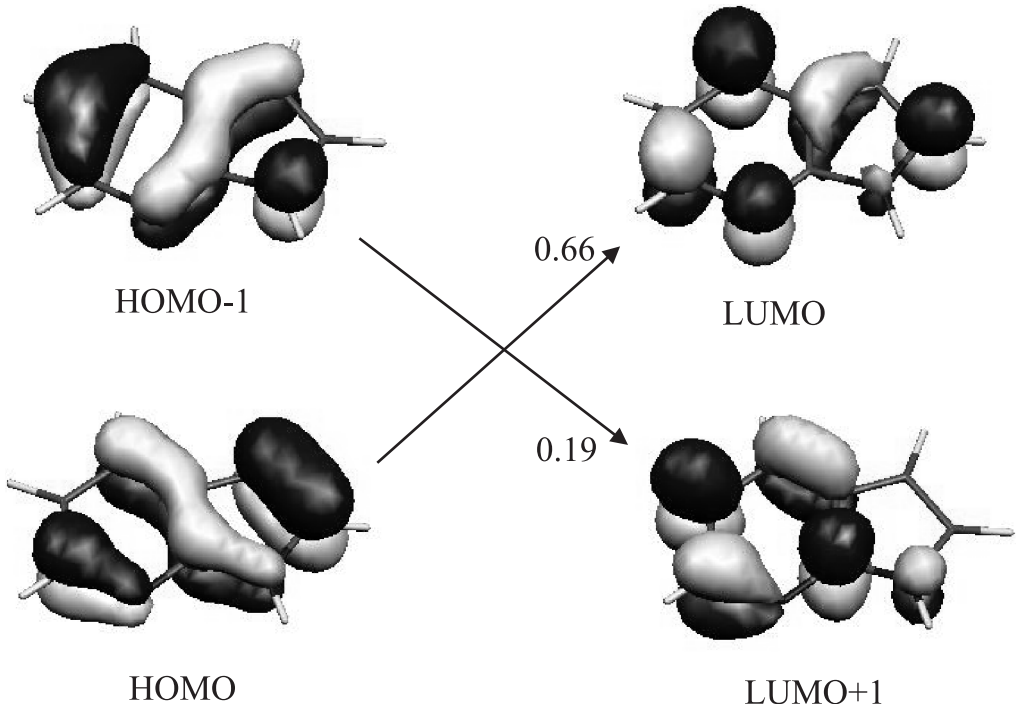

Figure 7. Molecular orbitals involved in the lowest ππ* transition.

Table 6. Experimental and *ab initio* inertial constants of 7AI. All calculations were performed using the 6-31G(d,p) basis set. All values are given in MHz.

	Exp.	MP2	HF	CIS	CIS-HF	CAS(12/10)[a]
A''	3928.93	3918	4022	–	–	3973[b]
B''	1702.629	1703	1722	–	–	1708[b]
C''	1188.128	1187	1206	–	–	1195[b]
A'	3745.56	–	–	3909	–	3782[c]
B'	1703.87	–	–	1712	–	1695[c]
C'	1171.51	–	–	1190	–	1170[c]
ΔA	−183.47	–	–	–	−113	−191
ΔB	1.24	–	–	–	−10	−13
ΔC	−16.62	–	–	–	−16	−25

[a]Values from forthcoming paper II.
[b]Geometry optimized to the S_0 state.
[c]Geometry optimized to the S_1 state.

ring of 7AI. The oscillator strength of this lowest ππ* transition is calculated to be 0.377.

The genetic algorithm-based fit also improves the accuracy of determination of parameters affecting the intensity, such as the orientation of the transition dipole moment, etc. From the relative TDM orientation of two different isotopomers we were able to determine the direction of the TDM in 7AI. The signed value of the transition dipole moment is found to be −21°. The CIS calculation for this transition gives a value of −19°. As can be inferred from figure 5, a negative angle θ of the TDM with the inertial a axis indicates that the TDM vector points in the direction of the pyrrolic NH group.

From the small isotopic origin shifts of all four isotopomers we conclude that the vibrational frequency changes of the CH and NH vibrations in 7AI upon deuteration are very similar in both electronic states.

The financial support of the Deutsche Forschungsgemeinschaft (SCHM 1043/9-4) is gratefully acknowledged. M.S. would like to thank the Nordrheinwestfälische Akademie der Wissenschaften for the grant which made this work possible. This work forms part of the PhD thesis of Christian Ratzer.

References

[1] Kasha, M., Horowitz, P., and El-Bayoumi, M. A., 1972, *Molecular Spectroscopy: Modern Research*, Vol. I (New York: Academic Press), p. 287.
[2] Smirnow, A. V., English, D. S., Rich, R. L., Lane, J., Teyton, L., Schwabacher, A. W., Luo, S., Thornburg, R. W., and Petrich, J. W., 1997, *J. phys. Chem.* B, **101,** 2758.
[3] Ilich, P., 1995, *J. Molec. Struct.*, **354,** 37.
[4] Shukla, M. K., and Mishra, P. C., 1998, *Chem. Phys.*, **230,** 187.
[5] Chaban, G. M., and Gordon, M. S., 1999, *J. phys. Chem.* A, **103,** 185.
[6] Graña, A. M., 1999, *J. Molec. Struct. Theochem.*, **466,** 145.
[7] Borin, A. C., and Serrano-Andrs, L., 2000, *Chem. Phys.*, **262,** 253.

[8] Caminati, W., di Bernardo, S., and Trombetti, A., 1990, *J. Molec. Struct.*, **223,** 415.
[9] Hassan, K. H., and Hollas, J. M., 1989, *J. Molec. Spectrosc.*, **138,** 398.
[10] Nakajima, A., Ono, F., Kihara, Y., Ogawa, A., Matsubara, K., Ishikawa, K., Baba, M., and Kaya, K., 1995, *Laser Chem.*, **15,** 167.
[11] Huang, Y., Arnold, S., and Sulkes, M., 1996, *J. phys. Chem.*, **100,** 4734.
[12] Catalán, J., and Pérez, P., 1979, *J. theor. Biol.*, **81,** 213.
[13] Hageman, J. A., Wehrens, R., de Gelder, R., Meerts, W. L., and Buydens, L. M. C., 2000, *J. chem. Phys.*, **113,** 7955.
[14] Meerts, W. L., Schmitt, M., and Groenenboom, G., 2004, *Can. J. Chem.*, **82** (in press).
[15] Schmitt, M., Küpper, J., Spangenberg, D., and Westphal, A., 2000, *Chem. Phys.*, **254,** 349.
[16] Suenram, R. D., Lovas, F. J., and Fraser, G. T., 1988, *J. Molec. Spectrosc.*, **127,** 472.
[17] Caminati, W., and di Bernardo, S., 1990, *J. Molec. Struct.*, **240,** 253.
[18] Gerstenkorn, S., and Luc, P., 1982, *Atlas du Spectre d'Absorption de la Molécule d'Iode* (Paris: CNRS).
[19] Levine, D., PGAPack V1.0, PgaPack can be obtained via anonymous ftp from: ftp://ftp.mcs.anl.gov/pub/pgapack/pgapack.tar.z
[20] Holland, J. H., 1975, *Adaption in Natural and Artificial Systems* (Ann Arbor, MI: The University of Michigan Press).
[21] Goldberg, D. E., 1989, *Genetic Algorithms in Search, Optimisation and Machine Learning* (Reading, MA: Addison-Wesley).
[22] Rechenberg, I., 1973, *Evolutionsstrategie – Optimierung Technischer Systeme nach Prinzipien der Biologischen Evolution* (Stuttgart: Frommann-Holzboog).
[23] Gray, F., 1953, Pulse Code Communication, U.S. Patent 2 632 058.
[24] Allen, H. C., and Cross, P. C., 1963, *Molecular Vib-Rotors* (New York: Wiley).
[25] Wu, Y. R., and Levy, D. H., 1989, *J. chem. Phys.*, **91,** 5278.
[26] Ratzer, C., Küpper, J., Spangenberg, D., and Schmitt, M., 2002, *Chem. Phys.*, **283,** 153.